Structural Engineering and Mechanics, *Vol. 62, No. 2 (2017) 125-138*
DOI: https://doi.org/10.12989/sem.2017.62.2.125

Reliability-based design optimization using reliability mapping functions

Weitao Zhao*, Xueyan Shi and Kai Tang

Key Laboratory of Liaoning Province for Composite Structural Analysis of Aerocraft and Simulation, Shenyang Aerospace University, Shenyang, 110-136, China

(Received August 11, 2016, Revised November 30, 2016, Accepted December 7, 2016)

Abstract. Reliability-based design optimization (RBDO) is a powerful tool for design optimization when considering probabilistic characteristics of design variables. However, it is often computationally intensive because of the coupling of reliability analysis and cost minimization. In this study, the concept of reliability mapping function is defined based on the relationship between the reliability index obtained by using the mean value first order reliability method and the failure probability obtained by using an improved response surface method. Double-loop involved in the classical RBDO can be converted into single-loop by using the reliability mapping function. Since the computational effort of the mean value first order reliability method is minimal, RBDO by using reliability mapping functions should be highly efficient. Engineering examples are given to demonstrate the efficiency and accuracy of the proposed method. Numerical results indicated that the proposed method has the similar accuracy as Monte Carlo simulation, and it can obviously reduce the computational effort.

Keywords: structural reliability; RBDO; reliability mapping function; response surface method

1. Introduction

Reliability-based design optimization (RBDO) is usually expressed in a form where one is required to minimize a cost function subjected to some reliability constraints and deterministic constraints. The reliability constraints ensure that failure probabilities with respect to various failure modes are below acceptable levels (Li 2013, Yuan and Lu 2014, Meng *et al.* 2015, Wang and Qiu 2015, Wang *et al.* 2014, Fang *et al.* 2013). Despite the advantages of RBDO, its application to practical engineering problem is still quite challenging (Yuan and Lu 2014). Both the optimization and reliability evaluation require repeated structural analyses for different values of design variables. Moreover, the evaluation of the structural response may be computationally costly, e.g., when the analysis of finite element model is involved. As a result, many approximate methods, such as double-loop methods (Grandhi and Wang 1998, Youn *et al.* 2005, Zhao and Qiu 2013), decoupled methods (Chen *et al.* 2013a, Du and Chen 2004, Cheng *et al.* 2006, Yi *et al.* 2008, Zou and Mahadevan 2006, Li *et al.* 2010, Cho and Lee 2011, Ching and Hsu 2008) and single-loop methods (Kirjner-Neto *et al.* 1998, Liang *et al.* 2008, Kharmanda *et al.* 2002, Shan and Wang 2008, Agarwal *et al.* 2007), have been proposed to alleviate the computational effort.

Double-loop method is achieved by a nested optimization process (Enevoldsen and Sorensen 1994, Tu *et al.* 1999). Design optimization loop (outer loop) is a deterministic optimization process; it repeatedly calls the reliability analysis loop (inner loop) in each cycle. Its computational effort is very high due to the multiplication of a number of iterations and structural analyses in both optimization and reliability analysis loop. Therefore, the double-loop method has some limitation in the use of practical application. Decoupling method is to transform the RBDO problem into a deterministic one by explicitly approximating the failure probability as a function of design variables (Gasser and Schueller 1997). The approximation of the failure probability occupies a considerable portion of the total computation effort in optimization procedure, because it needs a number of reliability analyses over various design variable values. One possible way of constructing the approximation is to adopt predefined function and select some predefined interpolation points in the space of the design variables. Single-loop method only has one loop during the design optimization process through replacing the reliability analysis with the Karush-Kuhn-Tucker optimality conditions (Kuschel and Rachwitz 1997). Thus, RBDO problems can be solved very efficiently for linear and weakly nonlinear problems (Chen *et al.* 2013b).

For solving RBDO problems, the failure probabilities are usually obtained by using standard reliability analysis methods like the first-order reliability method (FORM), the second-order reliability method (SORM), and Monte Carlo simulation (MCS) (Ditlevsen and Madsen 1996, Choi *et al.* 2007). The FORM usually contains three methods: the mean value FORM, Hasofer-Lind (HL) iteration method, and Rackwitz-Fiessler (RF) iteration method (Choi *et al.* 2007). HL and RF iteration methods are often called “Advanced FORM”. The mean value FORM is based on a linear approximation of the limit state function (LSF) at the mean point. The advanced FORM and SORM are based on linear and quadratic approximations of the LSFs at the Most Probable failure Point (MPP), respectively. The application

*Corresponding author, Associate Professor
E-mail: zhwt201@163.com

http://www.techno-press.org/?journal=sem&subpage=8 ISSN: 1225-4568 (Print), 1598-6217 (Online)

of advanced FORM and SORM requires the computation of the MPP by using iteration methods. The advanced FORM and SORM are perfectly adequate for linear LSFs and slightly nonlinear LSFs. However, the two methods are not accurate enough for highly nonlinear LSFs. MCS is an accurate technique to estimate the failure probability. Although it gives the exact solution, it is time-consuming for the large and complex structures with low failure probabilities and implicit LSFs. The mean value FORM is more efficient for reliability evaluation in terms of the total number of LSF evaluations because it needn't iteration computation, but it may be inaccurate for nonlinear LSFs. Nevertheless, the accurate failure probability is often highly correlated with the reliability index obtained by using the mean value FORM.

In this study, in order to reduce the computational effort of RBDO, the relationship between the reliability index obtained by using the mean value FORM and the failure probability obtained by using an accurate method is determined through a regression analysis. The relationship is called the reliability mapping function. Based on the reliability mapping function, an equivalent target reliability index corresponding to the mean value FORM can be determined so that the mean value FORM can be used for reliability evaluation in RBDO. Double-loop involved in the classical RBDO can be converted into single-loop by using the reliability mapping function. Since the computational effort involved in the mean value FORM is minimal, RBDO using the reliability mapping functions should be highly efficient in terms of the number of LSF evaluations.

2. Basic mathematical formulations

2.1 Reliability-based design optimization

The most basically mathematical formulation of RBDO problem is written as follows (Li 2013, Yuan and Lu 2014)

$$\begin{aligned} &\min\ C_0(\mathbf{d}) \\ &\text{s.t.}\ \ C_k = P[G_k(\mathbf{d},\mathbf{X}) \le 0] \le P_{fk}^c; k=1,\ldots,m \\ &\qquad \mathbf{d}^{\mathrm{L}} \le \mathbf{d} \le \mathbf{d}^{\mathrm{U}} \end{aligned} \tag{1}$$

where $C_0(\mathbf{d})$ is the objective function, C_k is the kth reliability constraint function, $\mathbf{X}$ is the vector of random variables, $\mathbf{d}$ is the vector of design variables, which can be physical quantities in the input parameters or distributional parameters of input random variables, G_k is the LSF for the kth reliability constraint, which defines the failure domain by $G_k(\mathbf{d},\mathbf{X}) \le 0$, P_{fk}^c is the target failure probability for the kth reliability constraint, $\mathbf{d}^{\mathrm{L}}$ and $\mathbf{d}^{\mathrm{U}}$ are allowable lower and upper bounds of $\mathbf{d}$, and m is the number of reliability constraints.

2.2 Mean value FORM

In the mean value FORM method, the LSF is represented as the first-order Taylor series expansion at the mean value point (Ditlevsen and Madsen 1996, Choi *et al.* 2007). Assuming that the random variables $\mathbf{X}$ are statistically independent, the approximate LSF at the mean is written as

$$\tilde{G}(\mathbf{X}) \approx G(\boldsymbol{\mu}_{\mathbf{X}}) + \nabla G(\boldsymbol{\mu}_{\mathbf{X}})^T (\mathbf{X} - \boldsymbol{\mu}_{\mathbf{X}}) \tag{2}$$

where $\mathbf{X}=\{x_1,x_2,\ldots,x_n\}^T$ is the vector of random variables, $\boldsymbol{\mu}_{\mathbf{X}} = \{\mu_{x_1},\mu_{x_2},\ldots,\mu_{x_n}\}^T$ is the mean value vector of random variables, n is the number of random variables, and $\nabla G(\boldsymbol{\mu}_{\mathbf{X}})$ is the gradient of LSF evaluated at $\boldsymbol{\mu}_{\mathbf{X}}$.

$$\nabla G(\boldsymbol{\mu}_{\mathbf{X}}) = \left\{ \frac{\partial G(\boldsymbol{\mu}_{\mathbf{X}})}{\partial x_1}, \frac{\partial G(\boldsymbol{\mu}_{\mathbf{X}})}{\partial x_2}, \ldots, \frac{\partial G(\boldsymbol{\mu}_{\mathbf{X}})}{\partial x_n} \right\}^T \tag{3}$$

The mean value of the approximate LSF $\tilde{G}(\mathbf{X})$ is

$$\mu_{\tilde{G}} = G(\boldsymbol{\mu}_{\mathbf{X}}) \tag{4}$$

The standard deviation of the approximate LSF $\tilde{G}(\mathbf{X})$ is

$$\sigma_{\tilde{G}} = \left[\left(\frac{\partial G(\boldsymbol{\mu}_{\mathbf{X}})}{\partial x_i} \right)^2 \sigma_{x_i}^2 \right]^{\frac{1}{2}} \tag{5}$$

where σ_{x_i} is the standard deviation of random variable x_i.

The reliability index β_M is computed as

$$\beta_M = \frac{\mu_{\tilde{G}}}{\sigma_{\tilde{G}}} \tag{6}$$

Since the approximate LSF is obtained by linearizing the original LSF at the mean value point, this method is called the mean value FORM. The β_M is called a mean value FORM reliability index. The mean value FORM is more efficient for reliability analysis because that it needn't iteration computation. In this study, the mean value FORM and the reliability mapping function are used for reliability evaluation in RBDO. Double-loop involved in the classical RBDO can be converted into single-loop by using the proposed method.

3. Definition of reliability mapping function

The mean value FORM is more efficient for reliability analysis, but it may be inaccurate. However, the accurate failure probability is often highly correlated with the mean value FORM reliability index β_M. The relationship between the mean value FORM reliability index β_M and the accurate failure probability is called the *reliability mapping function*. The reliability mapping function is shown in Fig. 1.

The reliability mapping function denoted by F is defined as

$$\beta_M = F(\beta_E) \tag{7}$$

where

$$\beta_E = \Phi^{-1}(1 - P_f) \tag{8}$$

where P_f is the failure probability obtained by using an

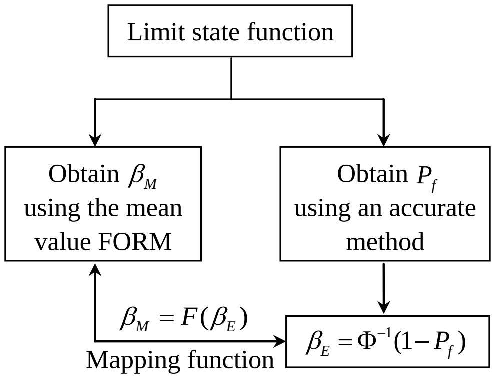

Fig. 1 Concept of reliability mapping function

accurate method, β_E is the generalized reliability index, and Φ^{-1} is the inverse of standard normal cumulative distribution function.

Substituting the target failure probability P_{fk}^c into Eq. (8) yields

$$\beta_{Ek}^c = \Phi^{-1}(1 - P_{fk}^c) \tag{9}$$

where β_{Ek}^c is the generalized target reliability index.

Substituting β_{Ek}^c into Eq. (7) yields

$$\beta_{Mk}^c = F(\beta_{Ek}^c) \tag{10}$$

where β_{Mk}^c is an equivalent target reliability index corresponding to the mean value FORM.

From Eqs. (9) and (10), Eq. (1) can be rewritten as

$$\begin{aligned} &\min\ C_0(\mathbf{d}) \\ &\text{s.t.}\ \ C_k = \beta_{Mk} \ge \beta_{Mk}^c ; k = 1, \ldots, m \\ &\qquad \mathbf{d}^{\mathrm{L}} \le \mathbf{d} \le \mathbf{d}^{\mathrm{U}} \end{aligned} \tag{11}$$

where β_{Mk} is a reliability index computed by using the mean value FORM for the kth reliability constraint, β_{Mk}^c is an equivalent target reliability index corresponding to the mean value FORM for the kth reliability constraint.

Since the mean value FORM needn't iteration computation, Eq. (11) is a single-loop problem. That is, Double-loop involved in the classical RBDO can be converted into single-loop by using reliability mapping functions.

4. Improved response surface method

As seen the above analysis in Section 3, the main challenge in the reliability mapping function is the calculation of the accurate failure probability. For this purpose, the improved RSM proposed by Zhao *et al.* (2016) is used, and the failure probability obtained by using the improved response surface method is utilized to construct the reliability mapping function. The algorithm of the improved response surface method (Zhao *et al.* 2016) has three stages. Firstly, some experimental points considering the region of main contribution to failure probability are selected based on the MPP; Secondly, a response function is construct to approximate the actual LSF; Thirdly, the MCS is utilized to evaluate the failure probability by using the response function.

4.1 Selection of experimental points

Based on the theory of structural reliability, the main contribution to failure probability comes from the region around the MPP (Zhao *et al.* 2016). The advanced FORM can find the MPP better. The algorithm of advanced FORM can be found in some textbooks (Ditlevsen and Madsen 1996, Choi *et al.* 2007). In this work, experimental points are selected based on the MPP so that the response function approximates the actual LSF better in the region around the MPP. The basic steps of the selection of experimental points are as follows:

1. Find the MPP using the advanced FORM.
2. Obtain the tangent hyperplane through the MPP in the standard normal space (U space). The expression of the tangent hyperplane is given by

$$(\mathbf{X} - \mathbf{X}_D)^T \boldsymbol{\omega} = 0 \tag{12}$$

where $\mathbf{X}_D$ is the MPP and $\boldsymbol{\omega}$ is the unit vector form the origin to $\mathbf{X}_D$.

3. Solve for a intersection point of the tangent hyperplane and the ith coordinate axis. The intersection points are denoted by $\mathbf{X}_i^c$ (i=1,2,…,n).
4. Select n experimental points along the direction form $\mathbf{X}_D$ to $\mathbf{X}_i^c$ in the standard normal space, as follows

$$\mathbf{X}_i^{(1)} = \mathbf{X}_D + f_1 \boldsymbol{\gamma}_i \qquad i = 1, 2, \ldots, n \tag{13}$$

where $\boldsymbol{\gamma}_i$ is the unit vector form the $\mathbf{X}_D$ to $\mathbf{X}_i^c$, and f_1 is an arbitrary factor.

5. Evaluate the LSF $G(\mathbf{X}_i^{(1)})$.
6. Select n experimental points in the standard normal space based on the values of $G(\mathbf{X}_i^{(1)})$, as follows

$$\mathbf{X}_i^{(2)} = \begin{cases} 0.5(\mathbf{X}_D + \mathbf{X}_i^{(1)}) + f_2 \boldsymbol{\omega} & G(\mathbf{X}_i^{(1)}) > 0 \\ 0.5(\mathbf{X}_D + \mathbf{X}_i^{(1)}) - f_2 \boldsymbol{\omega} & G(\mathbf{X}_i^{(1)}) < 0 \\ 0.5(\mathbf{X}_D + \mathbf{X}_i^{(1)}) & G(\mathbf{X}_i^{(1)}) = 0 \end{cases} \quad i = 1, 2, \ldots, n \tag{14}$$

where f_2 is an arbitrary factor.

The factors of f_1 and f_2 are selected as follows:

For a given importance level ε_p, the parameter ε_p is defined as

$$\Phi[-\beta(1 + \varepsilon_\beta)] = \varepsilon_p \Phi(-\beta) \tag{15}$$

where Φ is the standard normal cumulative distribution function, and β is the reliability index.

From Eq. (15), we have

$$\varepsilon_\beta = -\frac{\Phi^{-1}[\varepsilon_p \Phi(-\beta)]}{\beta} - 1 \tag{16}$$

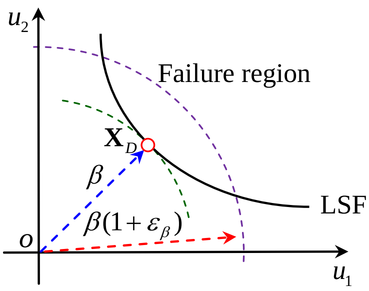

Fig. 2 The parameter ε_β in the two-dimensional standard normal space

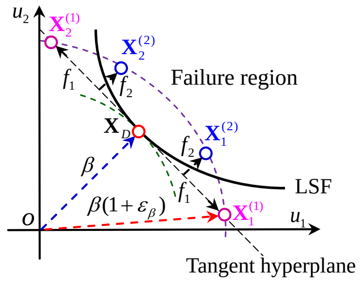

Fig. 3 Experimental points of the proposed method

In the two-dimensional standard normal space (U space), the parameter ε_β is shown in Fig. 2. Based on Eq. (15), the contribution to failure probability coming from the region, which is the region outside of β hypersphere and inside of $\beta(1+\varepsilon_p)$ hypersphere, should be 1-ε_p. For example, if the reliability index β=3, the failure probability $P_f=\Phi(-\beta)=\Phi(-3)$=1.3499×10^{-3}. For a given value of importance level ε_p=0.05, we have ε_β=0.2724. The failure probability $P_f^*=\Phi[-\beta(1+\varepsilon_\beta)]$=6.7495×10^{-5}, the ratio of $P_f^*/P_f=\varepsilon_p$=0.05. The contribution to failure probability coming from the region is $(P_f-P_f^*)/P_f$ =1-ε_p=95%. Therefore, for a given importance level ε_p, the parameter ε_β can define the size of main region influencing failure probability. In addition, the importance level ε_p characterizes the size of region of interest: lower it is, bigger is the region of interest. As seen from Eq. (15), the value of ε_p should be relatively low, such as 0.05. Actually, the importance level ε_p defines the region of interest outside of which the failure probability is considered as negligible.

Since the parameter ε_β can define the size of main region influencing failure probability, the factors of f_1 and f_2 are selected as

$$f_1=\sqrt{[\beta(1+\varepsilon_\beta)]^2-\beta^2} \tag{17}$$

$$f_2=0.5\beta\varepsilon_\beta \tag{18}$$

In the two-dimensional standard normal space, experimental points $\mathbf{X}_i^{(1)}$, $\mathbf{X}_i^{(2)}$ and $\mathbf{X}_D$ are shown in Fig. 3. As seen from Fig.3, experimental points of the proposed method can consider the size of main region influencing failure probability.

4.2 Response function

The experimental points $\mathbf{X}_i^{(1)}$, $\mathbf{X}_i^{(2)}$ and $\mathbf{X}_D$ are used to solve for the unknown coefficients of response function. Since these experimental points can consider the size of main region influencing failure probability, the fitting precision of the response function to the actual LSF in the region of interest is increased. The total number of experimental points used to construct the response function is 2n+1, thus a quadratic polynomial without cross terms is used as a response function, as follows

$$\bar{G}(\mathbf{X})=a+\sum_{i=1}^{n}b_i x_i+\sum_{i=1}^{n}c_i x_i^2 \tag{19}$$

where a, b_i and c_i are unknown coefficients, these unknown coefficients are obtained from the values of the LSF at experimental points.

4.3 Evaluation of failure probability

In the paper, the MCS is performed to evaluate the failure probability by using the response function. The failure probability P_f is given by

$$P_f=\frac{m_1}{N_s} \tag{20}$$

where N_s is the number of sample points for MCS, m_1 is the number of failure points.

Substituting P_f described by Eq. (20) into Eq. (8), the equivalent reliability index β_E can be obtained.

4.4 Discussion on accuracy and efficiency

Since the quadratic polynomial response function is used in the improved response surface method, the accuracy of the improved response surface method should be higher than that of the advanced FORM.

Since the improved response surface method is constructed based on the MPP resulting from the advanced FORM, the efficiency of the improved response surface method is slightly lower than that of the advanced FORM. As seen from experimental design, the total number of LSF evaluations of the improved response surface method is m_2+4n, where m_2 is the number of LSF evaluations used to obtain the MPP by using the advanced FORM, n is the number of random variables. The improved response surface method isn't used to solve RBDO problems directly, but it is used to construct reliability mapping functions. Thus, its efficiency is acceptable.

5. Construction of reliability mapping function

The regression analysis is used to construct the reliability mapping function. The basic steps are as follows:

1. Select a sample point corresponding to design variables in the design region.
2. Compute the MPP by using the advanced FORM.
3. Construct the response function based on the MPP.

4.Compute the failure probability P_f by using MCS in terms of the response function.

5. Compute the equivalent reliability index β_E by using the failure probability P_f.

6. Extract the reliability index β_M from the results of the advanced FORM.

7. Repeat steps 1-6 until enough data sets (β_E, β_M) are obtained.

8. Fit the relationship between β_E and β_M, i.e., obtain the reliability mapping function.

The first sample point $\mathbf{X}_S^{(1)}$ can be chosen with an appropriate engineering criterion. Subsequent sample points are determined as

$$\mathbf{X}_S^{(j)} = \mathbf{X}_S^{(j-1)}(1+\lambda^{(j)}\mathbf{S}^{(j)}) \tag{21}$$

where $\mathbf{X}_S^{(j)}$ is the jth sample point, $\mathbf{S}^{(j)}$ is the search direction vector, and $\lambda^{(j)}$ is the step size along the search direction.

The vector of $\mathbf{S}^{(j)}$ is determined by using the unit gradient of LSF evaluated at the sample point $\mathbf{X}_S^{(j)}$.

$$\mathbf{S}^{(j)} = \frac{\nabla G(\mathbf{X}_S^{(j)})}{\left\|\nabla G(\mathbf{X}_S^{(j)})\right\|} \tag{22}$$

where

$$\nabla G(\mathbf{X}_S^{(j)}) = \left\{\frac{\partial G(\mathbf{X}_S^{(j)})}{\partial d_1}, \frac{\partial G(\mathbf{X}_S^{(j)})}{\partial d_2}, \ldots, \frac{\partial G(\mathbf{X}_S^{(j)})}{\partial d_n}\right\}^T \tag{23}$$

Usually, if the mean value of LSF is increased, the reliability index will be increased for a given LSF. In addition, if design variables are not random variables, reliability sensitivities with respect to design variables will not be given directly in the process of reliability analysis. In this paper, the main objective is to construct the reliability mapping function. Thus, for the sake of simplicity, the unit gradient of the limit state function is used to determine $\mathbf{S}^{(j)}$.

The value of $\lambda^{(j)}$ can be chosen based on the value of β_E at jth sample point. If $\beta_E < \beta_E^c$, then $0<\lambda^{(j)}<1$; If $\beta_E > \beta_E^c$, then $-1<\lambda^{(j)}<0$. If the value of β_E is close to the generalized target reliability index β_E^c, then the small value of $\lambda^{(j)}$ will be chosen.

In order to obtain an accurate reliability mapping function using samples as few as possible, the criterion of enough data sets (β_E, β_M) is checked as follows: 1) at least two β_M in data sets (β_E, β_M) are greater than the generalized target reliability index β_E^c; 2) at least two β_M in data sets (β_E, β_M) are less than the generalized target reliability index β_E^c.

After enough data sets (β_E, β_M) are obtained, the functions of polyfit and polyconf in Matlab software are used. [p,s]=polyfit (β_E, β_M, h) returns a h-order polynomial, coefficients p and a structure s. [$\mathbf{z}$, Δz]=polyconf (p, β_E^c, s) takes outputs p and s from polyfit and generates a prediction interval [$\mathbf{z}-\Delta z$, $\mathbf{z}+\Delta z$] with a confidence level of 95% for a observation at the value of β_E^c. In this paper, the upper bound $z+\Delta z$ is used as a prediction value of the equivalent target reliability index in order to obtain relatively conservative optimization results, i.e., $\beta_M^c = z + \Delta z$.

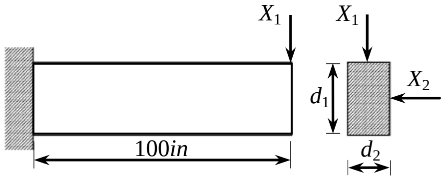

Fig. 4 Cantilever beam design problem

Table 1 Example 1-Statistical properties of random variables

Random variable	Mean value	Standard deviation	Distribution
X_1/lb	1000	100	Normal
X_2/lb	500	100	Normal
X_3/psi	4×10^4	2×10^3	Normal
X_4/psi	29×10^6	1.45×10^6	Normal

6. Examples

6.1 Example 1

The cantilever beam design is chosen as the first test problem as shown in Fig. 4. The RBDO problem can be formulated as follows (Li 2013)

$$\begin{aligned} &\min C_0(\mathbf{d}) = d_1 d_2 \\ &\text{s.t. } C_1 = P\left[X_3 - \frac{600}{d_1 d_2}\left(\frac{X_1}{d_2} + \frac{X_2}{d_1}\right) < 0\right] \le \Phi(-2.5) \\ &C_2 = P\left[2.5 - \frac{4\times10^6}{X_4 d_1 d_2}\sqrt{\frac{X_1^2}{d_2^4} + \frac{X_2^2}{d_1^4}} < 0\right] \le \Phi(-3.5) \\ &0 \le d_i \le 5; i = 1,2 \end{aligned} \tag{24}$$

where $\mathbf{d}$ is the vector of design variables, X_1 and X_2 are applied loads, X_3 is the yield stress, and X_4 is Young's modulus of the material. Their statistical properties are given in Table 1.

For this example, the first sample point is chosen as $\mathbf{X}_S^{(1)} = \{2,4\}^{\mathrm{T}}$. The corresponding β_E and β_M are calculated. The values of β_{E1} and β_{M1} are 0.5383 and 0.5382 with respect to LSF 1, and the values of β_{E2} and β_{M2} are 0.2126 and 0.2224 with respect to LSF 2, respectively. The value of β_{E1} is less than the generalized target reliability index $\beta_{E1}^c = 2.5$, and the value of β_{E2} is also less than the generalized target reliability index $\beta_{E2}^c = 3.5$. Thus, the value of $\lambda^{(1)}$ is chosen as 0.1 in this step. The unit gradients of LSF1 and LSF2 evaluated at the sample point $\mathbf{X}_S^{(1)}$ are $\{0.8944,\ 0.4472\}^T$ and $\{0.9656,\ 0.2600\}^T$, respectively. Since the two LSFs are considered in this example, the mean value of two unit gradients is used to compute the search direction vector $\mathbf{S}^{(1)}$, i.e., $\mathbf{S}^{(1)}=0.5\times(\{0.8944,\ 0.4472\}^T+\{0.9656,\ 0.2600\}^T)=\{0.9300,\ 0.3536\}^T$. The

Table 2 Example 1 - Reliability indices of sample points

Sample points		LSF1				LSF2			
d_1	d_2	β_M	β_{AF}	β_E	β_{MCS}	β_M	β_{AF}	β_E	β_{MCS}
2.0000	4.0000	0.5382	0.5382	0.5383	0.5385	0.2224	0.2209	0.2126	0.2129
2.1860	4.1414	2.2269	2.2267	2.2268	2.2268	2.2788	2.1356	2.1286	2.1290
2.3867	4.3004	4.1143	4.1139	4.1142	4.1141	5.1637	4.4699	4.4402	4.4405
2.2787	4.0288	2.4485	2.4483	2.4484	2.4486	2.9733	2.7198	2.6958	2.7063
2.3812	4.1149	3.4237	3.4234	3.4228	3.4226	4.4873	3.9332	3.8967	3.9091

second sample point $\mathbf{X}_S^{(2)} = \mathbf{X}_S^{(1)}(1+\lambda^{(1)}\mathbf{S}^{(1)})$ ={2.1860, 4.1414}$^{\mathrm{T}}$. The corresponding β_E and β_M are calculated repeated at the second sample point. The values of β_{E1} and β_{M1} are 2.2268 and 2.2269 with respect to LSF 1, and the values of β_{E2} and β_{M2} are 2.1286 and 2.2788 with respect to LSF 2, respectively. The values of β_{E1} and β_{E2} are both less than the generalized target reliability indices, thus the value of $\lambda^{(2)}$ is chosen as 0.1 in this step. The unit gradients of LSF1 and LSF2 evaluated at the sample point $\mathbf{X}_S^{(2)}$ are {0.8808, 0.4734}$^{\mathrm{T}}$ and {0.9557, 0.2943}^{T}, respectively. Thus, the search direction vector $\mathbf{S}^{(2)}$={0.9183, 0.3839}^{T}, and the third sample point $\mathbf{X}_S^{(3)} = \mathbf{X}_S^{(2)}(1+\lambda^{(2)}\mathbf{S}^{(2)})$ ={2.3867, 4.3004}^{T}. The above steps are repeated until enough data sets (β_E, β_M) are obtained.

Data sets (β_E, β_M) are listed in Table 2. In Table 2, β_{AF} is the reliability index obtained by using the advanced FORM, and β_{MCS} is the generalized reliability index obtained by using the MSC with 10^6 samples. As seen from Table 2, all β_E are close to β_{MCS}, that is, the accuracy of the proposed improved response surface method is enough. Compared with the advanced FORM, the proposed improved response surface method is more accurate.

The relationships between β_E and β_M are shown in Fig. 5, a linear and a quadratic polynomials are used to construct reliability mapping functions, as follows:

LSF1:

$$\beta_{M1} = 1.00015\beta_{E1} - 0.00016 \tag{25}$$

LSF2:

$$\beta_{M2} = 0.03857\beta_{E2}^2 + 0.99404\beta_{E2} + 0.05729 \tag{26}$$

Substituting the target reliability index $\beta_{E1}^c = 2.5$ into Eq. (25), a prediction interval [2.5002-0.0013, 2.5002+0.0013] with a confidence level of 95% are obtained. Thus, β_{M1}^c =2.5002 +0.0013=2.5015. Similarly, substituting the target reliability index $\beta_{E2}^c = 3.5$ into Eq. (26) yields β_{M2}^c =3.9573+0.1177=4.0750.

Based on reliability mapping functions, Eq. (24) can be rewritten as

$$\begin{aligned} &\min\ C_0(\mathbf{d}) = d_1 d_2 \\ &\text{s.t.}\ \ C_1 = \beta_{M1} \geq \beta_{M1}^c = 2.5015 \\ &\qquad C_2 = \beta_{M2} \geq \beta_{M2}^c = 4.0750 \\ &\qquad 0 \leq d_i \leq 5;\ i = 1,2 \end{aligned} \tag{27}$$

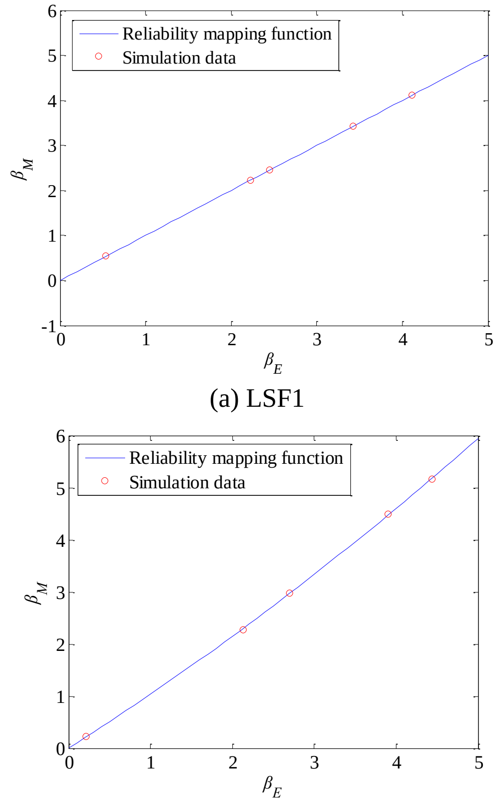

(a) LSF1

(b) LSF2

Fig. 5 Reliability mapping functions (Example 1)

As seen from Eq. (27), double-loop involved in the classical RBDO can be converted into single-loop by using reliability mapping functions.

The same optimization algorithm (sequential quadratic programming) and initial design ($\mathbf{d}_0$={2,4}^{T}) as the study of Li (2013) are selected in this example. Optimization results by using various methods for the cantilever beam are listed in Table 3. In Table 3, $\mathbf{d}^* = \{d_1^*, d_2^*\}^{\mathrm{T}}$ expresses the optimal design. As seen from Table 3, the results show that all methods attain the same optimum value (≈9.21) of the objective function. The proposed method is satisfactory in terms of the total number of LSF evaluations, optimal design, constraints and objective function. Compared with the advanced FORM, the proposed method can obviously reduce the total number of LSF evaluations as the result of using reliability mapping functions.

The constraints associated with the optimal design generated by each method are evaluated by using the MCS

Table 3 Example 1 - Optimization results

	Advanced FORM (Li 2013)	Li (2013)	Proposed method	Monte Carlo (Li 2013)
No. of iterations	7	6	6	7
No. of LSF evaluations	1900	302	294	29×106
d_1^*	2.4533	2.4588	2.4621	2.4629
d_2^*	3.7545	3.7462	3.7412	3.7403
$\frac{[C_1(\mathbf{d}^*)-\Phi(-2.5)]}{\Phi(-2.5)}$	0.01 %	-0.02%	-0.01%	-0.08%
$\frac{[C_2(\mathbf{d}^*)-\Phi(-3.5)]}{\Phi(-3.5)}$	7.51%	-4.13%	-2.23%	1.03%
$C_0(\mathbf{d}^*)$	9.2109	9.2115	9.2112	9.2119

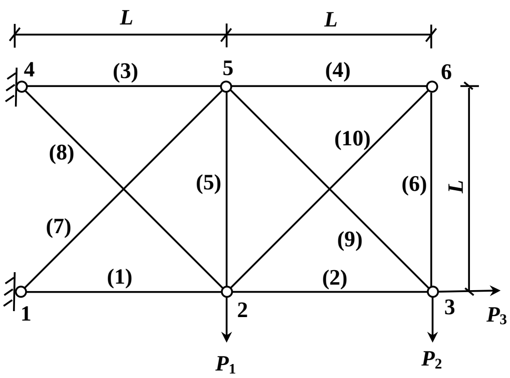

Fig. 6 A 10-bar truss structure

(10^6 samples), and the results are also listed in Table 3. It appears that the advanced FORM slightly violates the second constraint with a maximum error of 7.51% in calculating the failure probability. In contrast, no such violations are observed in the proposed method. This is because 1) the proposed improved response surface method is more accurate than the advanced FORM in performing reliability analysis; 2) the upper bound of prediction interval is used as a prediction value of the equivalent target reliability index in order to obtain relatively conservative optimization results.

6.2 Example 2

A 10-bar structure (Yuan and Lu 2014) is considered which is shown in Fig. 6. The length of all the horizontal and vertical bars is L. P_i (i=1,2,3) are loads. The section area and Young's modulus of each bar are A_i (i=1,2,…,10) and E, respectively. The fifteen random variables, i.e.

$$\mathbf{X}=\{A_1,A_2,A_3,A_4,A_5,A_6,A_7,A_8,A_9,A_{10},L,E,P_1,P_2,P_3\}^T \quad (28)$$

are all normally distributed and their distribution information is given in Table 4.

The means of L and A_i (i=1,2,…,10) are taken as design variables, i.e.

$$\mathbf{d}=\{\mu_{A_1},\mu_{A_2},\mu_{A_3},\mu_{A_4},\mu_{A_5},\mu_{A_6},\mu_{A_7},\mu_{A_8},\mu_{A_9},\mu_{A_{10}},\mu_L\}^T \quad (29)$$

The optimization model is given by

Table 4 Example2-Statistical properties of random variables

Random variable	Mean value	Coefficient of variance	Distribution
A_i/cm^2	μ_{A_i}	0.1	Normal
L/m	μ_L	0.1	Normal
E/Gpa	70	0.1	Normal
P_1/kN	500	0.2	Normal
P_2/kN	100	0.2	Normal
P_3/kN	100	0.2	Normal

Table 5 Example 2-Reliability indices of sample points

Sample points	β_M	β_{AF}	β_E	β_{MCS}
$\{8,8,8,8,8,8,8,8,8,8,1.6\}^T$	3.2245	2.5720	2.5286	2.5284
$\{8.7097,7.9904,8.7747,8.0078,7.9884,8.0078,8.5351,8.6651,8.1940,8.0221,1.3083\}^T$	5.7209	3.9469	4.0118	4.0128
$\{8.3843,7.9950,8.4276,8.0041,7.9945,8.0041,8.2894,8.3585,8.0993,8.0116,1.4419\}^T$	4.4534	3.2995	3.2386	3.2389
$\{8.0430,7.9998,8.0598,8.0002,8.0005,8.0002,8.0315,8.0375,8.0026,8.0007,1.5823\}^T$	3.3519	2.6526	2.6069	2.6075
$\{8.2198,7.9974,8.2524,8.0022,7.9976,8.0022,8.1651,8.2033,8.0512,8.0062,1.5096\}^T$	3.8975	2.9838	2.9540	2.9537

$$\begin{aligned}
&\min C_0(\mathbf{d})=\mu_L\left(\sum_{i=1}^{6}\mu_{A_i}+\sqrt{2}\sum_{i=7}^{10}\mu_{A_i}\right)\\
&\text{s.t. } C_1=P\left[D-d_y(\mathbf{X})\right]\le 10^{-3}\\
&\quad 1.3\le \mu_L\le 1.7\\
&\quad 6\le \mu_{A_i}\le 10\ \ (i=1,2,\dots,10)
\end{aligned} \quad (30)$$

where $C_0(\mathbf{d})$ is the objective function represents the volume of the 10-bar structure, D=0.1 m, and $d_y(\mathbf{X})$ is the displacement of Node 3 in vertical direction.

Data sets (β_E, β_M) are listed in Table 5. As seen from Table 5, all β_E are close to β_{MCS}, that is, the accuracy of the proposed improved response surface method is enough. Compared with advanced FORM, the proposed improved response surface is more accurate.

The relationship between β_E and β_M is shown in Fig. 7, a linear polynomial is used to construct a reliability mapping function, as follows

$$\beta_M = 1.69196\beta_E - 1.06127 \quad (31)$$

Substituting the target reliability index $\beta_E^c=\Phi^{-1}(1-10^{-3})$

Table 6 Example 2 - Optimization results

	No. of iterations	No. of LSF evaluations	$C_0(\mathbf{d}^*)$	$\frac{[C_1(\mathbf{d}^*)-10^{-3}]}{10^{-3}}$	$\mathbf{d}^*$
Advanced FORM	14	3772	98.1930	7.3%	$\{6.8083,6,8.0374,6,6,6,8.4113,6,6,6,1.3\}^T$
Yuan and Lu (2014)	13	2.6×104	99.0155	18.1%	$\{6.5887,6,8.6081,6,6,6,8.1410,6,6,6,1.3\}^T$
Proposed method	14	1114	98.6657	-5.8%	$\{6.9435,6,8.0505,6,6,6,8.5707,6,6,6,1.3\}^T$

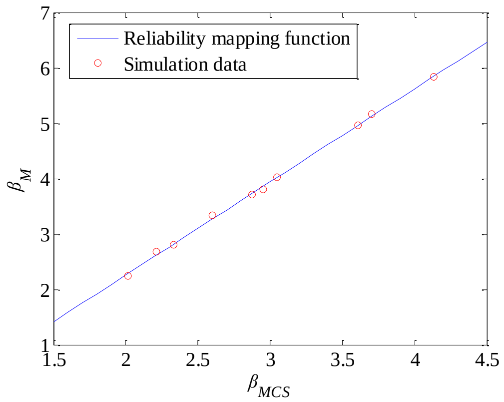

Fig. 8 Reliability mapping function based on MCS (Example 2)

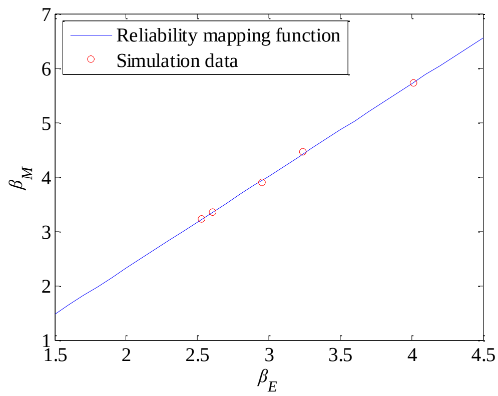

Fig. 7 Reliability mapping function (Example 2)

=3.0902 into Eq. (31), a prediction interval [4.1672-0.1078, 4.1672+0.1078] with a confidence level of 95% is obtained. Thus, β_M^c = 4.1672+0.1078 = 4.2750.

Based on the reliability mapping function, Eq. (30) can be rewritten as

$$\begin{aligned} &\min C_0(\mathbf{d}) = \mu_L\left(\sum_{i=1}^{6}\mu_{A_i} + \sqrt{2}\sum_{i=7}^{10}\mu_{A_i}\right) \\ &\text{s.t. } C_1 = \beta_M \ge \beta_M^c = 4.2750 \\ &\qquad 1.3 \le \mu_L \le 1.7 \\ &\qquad 6 \le \mu_{A_i} \le 10 \ \ (i = 1, 2, \ldots, 10) \end{aligned} \tag{32}$$

The same optimization algorithm (sequential quadratic programming) and initial design ($\mathbf{d}_0$={10,10,10,10,10,10, 10, 10,10,10,1.7}$^{\mathrm{T}}$) as the study of Yuan and Lu (2014) are adopted in this example. Optimization results obtained by using various methods are listed in Table 6. The constraint associated with the optimal design generated by each method is evaluated by using MCS (10^6 samples), and the results are also listed in Table 6. As seen from Table 6, the proposed method does not excessively violate the constraint in calculating the failure probability, that is, the accuracy of the proposed method is enough. Compared with the advanced FORM, the proposed method is more effective and accurate in terms of LSF evaluations and constraint. The proposed method can obviously reduce the total number of LSF evaluations, that is, the proposed method can obviously alleviate the computational effort for RBDO problems. Compared with the study of Yuan and Lu (2014), the proposed method is more effective and accurate. But, the advantage of the study of Yuan and Lu (2014) is also obvious as it needs only one reliability analysis and it seems insensitive to the number of design variables.

In order to investigate the effect of sample points on the construction of reliability mapping function, 10 sample points are selected randomly from the design space. The corresponding reliability indices β_M and β_{MCS} are computed by using the mean value FORM and the MCS with 10^6 samples. The relationship between β_M and β_{MCS}, i.e., the reliability mapping function based on MCS is shown in Fig. 8. A prediction value of β_M^c =4.2733 is obtained, the corresponding optimum value of the objective function is 98.6670, and the corresponding optimal design is {6.9446,6,8.0509,6,6,6,8.5718,6,6,6,1.3}$^{\mathrm{T}}$. Compared with results in Table 6, the consistent results are obtained, that is, the reliability mapping function does not depend on the selection of sample points, and the use of reliability mapping function to solve RBDO problem is feasible. In addition, the consistent results also indicate that the accuracy of proposed method is enough.

6.3 Example 3

A rod of circular cross-section is considered, it is subjected to a tensile force *P*, and its radius is *r*. The yield stress is σ_y. Three random variables X={σ_y,*P*,*r*}^{T}are considered, and their means and standard deviations are given in Table 7. The mean of *r* is taken as a design variable, i.e., $d=\mu_r$. The optimization model based on the static-strength reliability is given by

$$\begin{aligned} &\min C_0(\mathbf{d}) = \pi\mu_r^2 \\ &\text{s.t. } C_1 = P\left[G(\mathbf{X},\mathbf{d}) \le 0\right] \le \Phi(-3.0) \\ &\qquad 8 \le \mu_r \le 12 \end{aligned} \tag{33}$$

Table 7 Example 3-Statistical properties of random variables

Random variable	Mean value	Standard deviation
X_1/MPa	360	36
X_2/kN	200	20
X_3/mm	μ_r	2

Table 8 Example 3 - Six Cases

	LSF	Distribution		
		X_1	X_2	X_3
Case 1	Eq.(34)	Normal	Normal	Normal
Case 2	Eq.(35)	Normal	Normal	Normal
Case 3	Eq.(34)	Normal	Normal	Gumbel
Case 4	Eq.(35)	Normal	Normal	Gumbel
Case 5	Eq.(34)	Lognormal	Normal	Gumbel
Case 6	Eq.(35)	Lognormal	Normal	Gumbel

where $C_0(\mathbf{d})$ is the objective function represents the area of the rod.

It has been well known that the reliability indices obtained by the mean value FORM are usually different in terms of different LSFs with the same physical meaning. Thus, two LSFs with the same physical meaning are discussed, the one is

$$G(\mathbf{X},\mathbf{d}) = \sigma_s - \frac{P}{\pi r^2} \tag{34}$$

the other is

$$G(\mathbf{X},\mathbf{d}) = \sigma_s \pi r^2 - P \tag{35}$$

In addition, distribution types of random variables have an important effect on the reliability. Therefore, the different distribution types of random variables are also discussed in this example. Six Cases are listed in Table 8.

Since the only one design variable $d=\mu_r$ is considered, five sample points used to construct reliability mapping function are uniformly selected from interval [8,12]. The calculation results of reliability indices of sample points, reliability mapping functions and prediction values of β_M^c are all listed in Table 9. The reliability mapping functions of six Cases are shown in Fig. 9. As seen from Table 9 and Fig. 9, the reliability indices of sample points, reliability mapping functions and prediction values of β_M^c are all different in terms of six Cases. The main reason is follows: the reliability indices obtained by the mean value FORM are usually different in terms of different LSFs with the same physical meaning.

Since the only one design variable $d=\mu_r$ is considered, the brute-force approach is adopted to obtain the optimal solution. That is, the 10^5 points are uniformly selected from interval [8,12], and at each point, the failure probability is estimated by direct MCS with 10^6 samples. Optimization results obtained by using various methods in terms of six Cases are all listed in Table 10. As seen from Table 10, for six Cases, the optimal solutions obtained by using the

Table 9 Example 3 - Calculation results

Sample points		8	9	10	11	12	Reliability mapping functions and β_M^c
Case 1	β_M	4.3225	5.7005	6.8146	7.6343	8.2118	$\beta_M = -0.54818\beta_E^2 + 5.10629\beta_E - 3.33469$
	β_{AF}	1.8857	2.3824	2.8793	3.3759	3.8732	β_M^c =7.1069
	β_E	1.8792	2.3736	2.8715	3.3689	3.8586	
	β_{MCS}	1.8774	2.3718	2.8707	3.3674	3.8552	
Case 2	β_M	1.4264	1.7247	2.0068	2.2761	2.534	$\beta_M = 0.55878\beta_E + 0.38990$
	β_{AF}	1.8857	2.3825	2.8793	3.3761	3.8727	β_M^c =2.1134
	β_E	1.8791	2.3733	2.8719	3.3683	3.8572	
	β_{MCS}	1.8774	2.3718	2.8707	3.3674	3.8552	
Case 3	β_M	4.3312	5.7091	6.8224	7.6413	8.2181	$\beta_M = -0.55021\beta_E^2 + 5.11563\beta_E - 3.33801$
	β_{AF}	1.8911	2.3878	2.8847	3.3813	3.8788	β_M^c =7.1147
	β_E	1.8786	2.3775	2.8698	3.3684	3.8656	
	β_{MCS}	1.8765	2.3751	2.8693	3.3655	3.8638	
Case 4	β_M	1.4291	1.7271	2.0089	2.2779	2.5358	$\beta_M = 0.55654\beta_E + 0.39705$
	β_{AF}	1.8911	2.3879	2.8847	3.3815	3.8783	β_M^c =2.1176
	β_E	1.8786	2.3784	2.8705	3.3687	3.8668	
	β_{MCS}	1.8765	2.3751	2.8693	3.3655	3.8638	
Case 5	β_M	4.3055	5.6804	6.7931	7.6121	8.1894	$\beta_M = -0.54259\beta_E^2 + 5.07188\beta_E - 3.31140$
	β_{AF}	1.8861	2.3829	2.8801	3.3765	3.8739	β_M^c =7.0457
	β_E	1.8797	2.3786	2.8765	3.3681	3.8674	
	β_{MCS}	1.8786	2.3762	2.8719	3.3675	3.8656	
Case 6	β_M	1.4196	1.7164	1.9972	2.2651	2.5221	$\beta_M = 0.55444\beta_E + 0.39063$
	β_{AF}	1.8861	2.3831	2.8801	3.3771	3.8741	β_M^c =2.1025
	β_E	1.8795	2.3784	2.8751	3.3695	3.8673	
	β_{MCS}	1.8786	2.3762	2.8719	3.3675	3.8656	

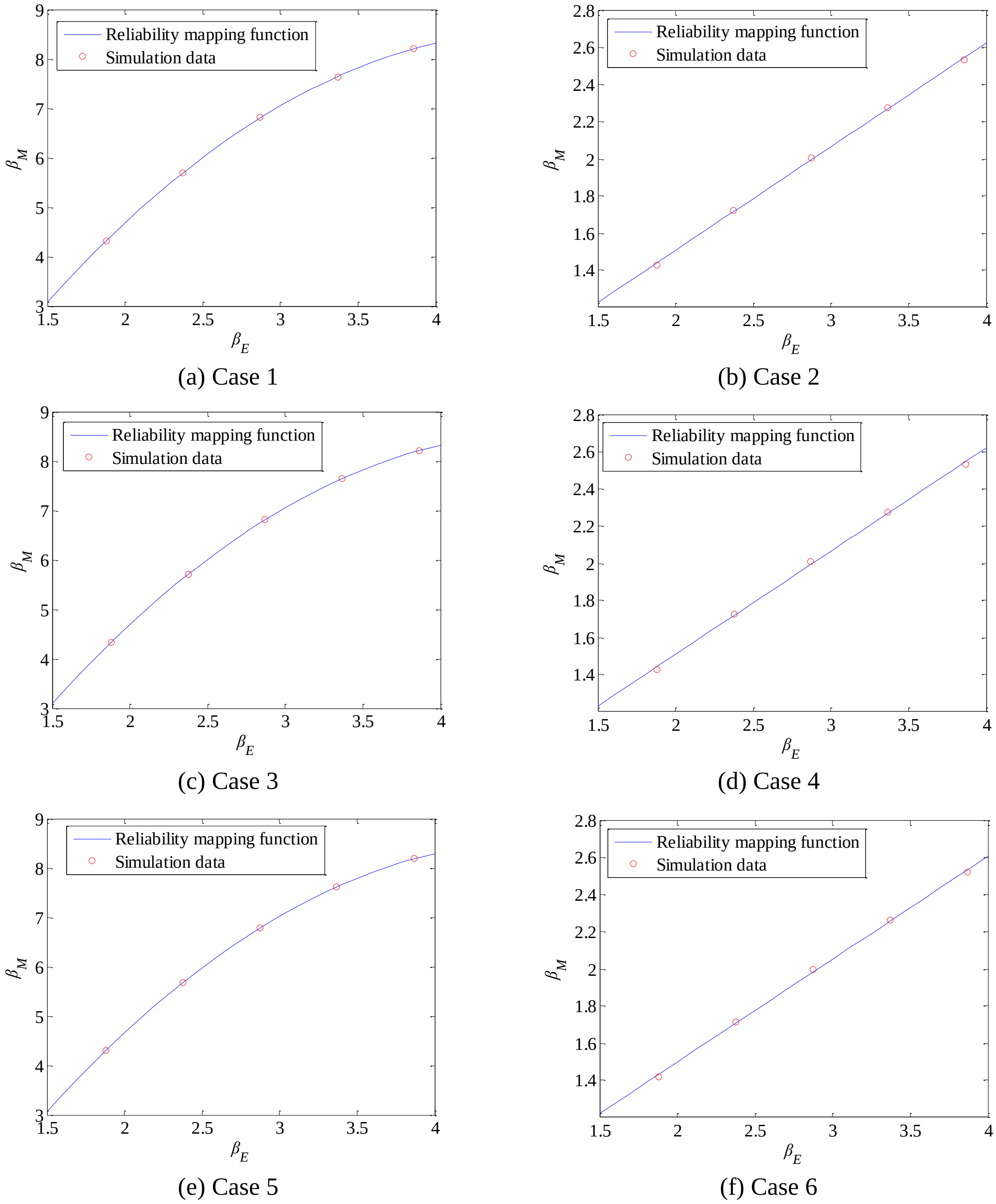

(a) Case 1 (b) Case 2

(c) Case 3 (d) Case 4

(e) Case 5 (f) Case 6

Fig. 9 Reliability mapping functions (Example 3)

proposed method are all close to the those obtained by using MCS. Compared with Case 1 and 2, Case 3 and 4, and Case 5 and 6, the consistent results are obtained. That is, the use of reliability mapping function to solve RBDO problems is feasible even thought the different LSFs with the same physical meaning are used to construct the reliability mapping function. In addition, for non-normally distributed random variables, the proposed method can also obtain satisfying results. This illustrates the robustness of the proposed method in solving the RBDO problems.

6.4 Example 4

A 72-bar space truss structure (Ho-Huu *et al*. 2016) shown in Fig. 10 is considered. The weight of the truss is the objective function and cross-sectional area for the truss members are defined as design variables. The density and Young's modulus of material are 0.1 lb/in^3 and E, respectively. Design variables are collected in 16 groups as shown in Table 11. Loads are applied at Node 1 with value 5 kips in x direction, 5 kips in y direction and -5 kips in z direction, respectively. Therefore, this RBDO problem involves 16 design variables $\mathbf{d}=\{\mu_{A_1},\mu_{A_2},\ldots,\mu_{A_{16}}\}^T$ and 20 random variables $\mathbf{X}=\{A_1,A_2,\ldots,A_{16},E,P_x,P_y,P_z\}^T$. The minimum and maximum cross-sectional area of each member are set to 0.1 and 4.5 in^2, respectively. The displacement limits at Node 1 in x and y directions are both ±0.25in. The probabilistic constraints, subjected to displacement limitations at Node 1 in x and y directions, are both not less than 99.865%, i.e., β^c=3.0.

Table 10 Example 3 - Optimization results

	Method	$\mathbf{d}^*$	$C_0(\mathbf{d}^*)$	$[C_1(\mathbf{d}^*)-\Phi(-3.0)]/\Phi(-3.0)$
Case 1	Advanced FORM	10.2433	329.63	-0.06%
	Proposed method	10.2415	329.51	0.03%
	MCS	10.2422	329.56	0.01%
Case 2	Advanced FORM	10.2430	329.61	-0.05%
	Proposed method	10.2413	329.50	0.03%
	MCS	10.2421	329.55	0.02%
Case 3	Advanced FORM	10.2323	328.92	-0.05%
	Proposed method	10.2310	328.84	-0.02%
	MCS	10.2302	328.79	0.01%
Case 4	Advanced FORM	10.2320	328.90	-0.05%
	Proposed method	10.2309	328.83	-0.01%
	MCS	10.2305	328.81	0.01%
Case 5	Advanced FORM	10.2414	329.51	-0.06%
	Proposed method	10.2401	329.43	-0.02%
	MCS	10.2387	329.34	0.01%
Case 6	Advanced FORM	10.2413	329.50	-0.06%
	Proposed method	10.2396	329.39	-0.02%
	MCS	10.2385	329.32	-0.01%

In order to further verify the robustness and efficiency of the proposed method, two Cases listed in Table 12 are discussed. Case 1: all random variables follow normal distribution. Case 2: P_x, P_y, P_z and E follow lognormal distribution, and A_i follow normal distribution.

The results of example 2 indicated that the reliability mapping function does not depend on the selection of sample points. Thus, for the sake of simplicity, five sample points used to construct reliability mapping function are uniformly selected from interval [0.8,1.2] in terms of all design variables. But, it is noted that the choice strategy of sample points presented in this paper is more efficient than the one of random selection, the results of example 2 has confirmed it. The calculation results of reliability indices of sample points, reliability mapping functions and prediction values of β_M^c are listed in Tables 13 and 14. The reliability mapping functions under two Cases are shown in Fig. 11.

The sequential quadratic programming with an initial design $\mathbf{d}_0=\{2.3,2.3,\ldots,2.3\}^{\mathrm{T}}$ is adopted in this example. Optimization results obtained by using various methods are listed in Table 15. The constraints associated with the optimal design generated by each method are evaluated by using MCS (10^6 samples), and the results are also listed in Table 15.

As seen from Table 15, the proposed method can obtain

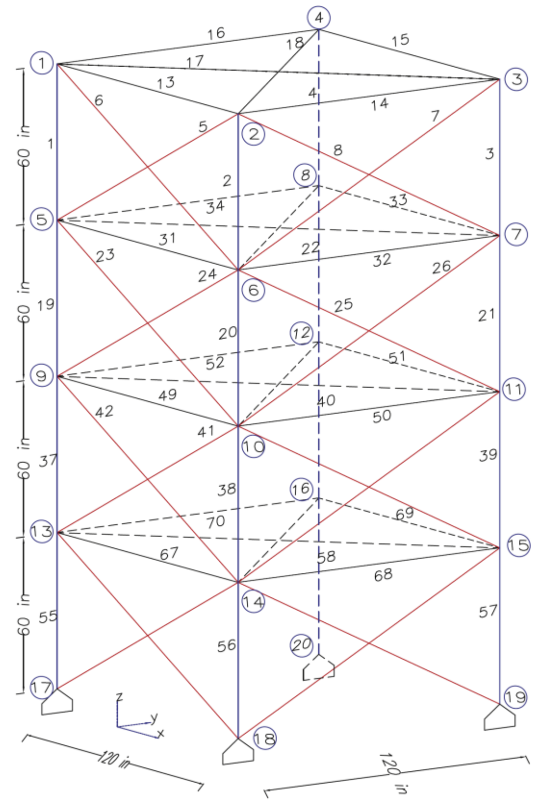

Fig. 10 The 72-bars pace truss structure (Example 4)

Table 11 Example 4 - Group assignments for members of 72-bar truss

Area group	Truss members
A_1	1, 2, 3, 4
A_2	5, 6, 7, 8, 9, 10, 11, 12
A_3	13, 14, 15, 16
A_4	17, 18
A_5	19, 20, 21, 22
A_6	23, 24, 25, 26, 27, 28, 29, 30
A_7	31, 32, 33, 34
A_8	35, 36
A_9	37, 38, 39, 40
A_{10}	41, 42, 43, 44, 45, 46, 47, 48
A_{11}	49, 50, 51, 52
A_{12}	53, 54
A_{13}	55, 56, 57, 58
A_{14}	59, 60, 61, 62, 63, 64, 65, 66
A_{15}	67, 68, 69, 70
A_{16}	71, 72

Table 12 Example 4 - Statistical properties of random variables

Random variable	Mean value	Coefficient of variance	Distribution	
			Case 1	Case 2
A_i/in^2	μ_{A_i}	0.05	Normal	Normal
E/ksi	10^4	0.05	Normal	Lognormal
P_x/kip	5	0.05	Normal	Lognormal
P_y/kip	5	0.05	Normal	Lognormal
P_z/kip	-5	0.05	Normal	Lognormal

Table 13 Example 4- Calculation results (Case 1)

Sample points	LSF1				LSF2			
	β_M	β_{AF}	β_E	β_{MCS}	β_M	β_{AF}	β_E	β_{MCS}
$\{0.8,0.8,...,0.8\}^T$	0.4180	0.4075	0.4124	0.4123	0.418	0.4075	0.4123	0.4126
$\{0.9,0.9,...,0.9\}^T$	1.8055	1.6893	1.7096	1.7101	1.8055	1.6893	1.7096	1.7102
$\{1.0,1.0,...,1.0\}^T$	3.1931	2.8656	2.8999	2.9003	3.1931	2.8656	2.9000	2.9004
$\{1.1,1.1,...,1.1\}^T$	4.5806	3.9424	3.9897	3.9899	4.5806	3.9424	3.9896	3.9891
$\{1.2,1.2,...,1.2\}^T$	5.9682	4.9271	4.9862	4.9836	5.9682	4.9271	4.9863	4.9872
Reliability mapping functions and β_M^c	$\beta_M = 0.04646\beta_E^2 + 0.96055\beta_E + 0.01810$ β_M^c =3.3734				$\beta_M = 0.04648\beta_E^2 + 0.96051\beta_E + 0.01819$ β_M^c =3.3728			

Table 14 Example 4- Calculation results (Case 2)

Sample points	LSF1				LSF2			
	β_M	β_{AF}	β_E	β_{MCS}	β_M	β_{AF}	β_E	β_{MCS}
$\{0.8,0.8,...,0.8\}^T$	0.4184	0.4064	0.4084	0.4083	0.4184	0.4064	0.4084	0.4083
$\{0.9,0.9,...,0.9\}^T$	1.8067	1.6709	1.6792	1.6789	1.8067	1.6709	1.6793	1.6791
$\{1.0,1.0,...,1.0\}^T$	3.1951	2.8226	2.8367	2.8359	3.1951	2.8226	2.8367	2.8354
$\{1.1,1.1,...,1.1\}^T$	4.5835	3.8796	3.899	3.8993	4.5835	3.8796	3.8989	3.8987
$\{1.2,1.2,...,1.2\}^T$	5.9719	4.8559	4.8802	4.8806	5.9719	4.8559	4.8803	4.881
Reliability mapping functions and β_M^c	$\beta_M = 0.04746\beta_E^2 + 0.98252\beta_E + 0.00904$ β_M^c =3.4090				$\beta_M = 0.04744\beta_E^2 + 0.98259\beta_E + 0.00896$ β_M^c =3.4082			

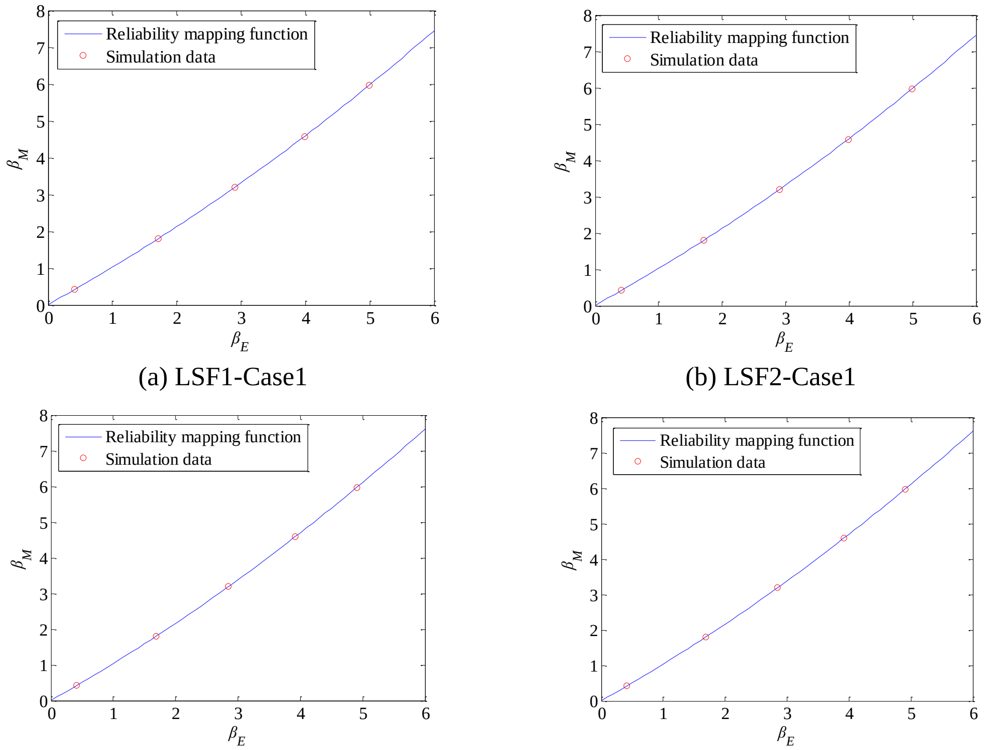

(a) LSF1-Case1 (b) LSF2-Case1

(c) LSF1-Case2 (d) LSF2-Case2

Fig. 11 Reliability mapping functions (Example 4)

satisfying results in terms of LSF evaluations and constraints. For Case 1, the results obtained by using the proposed method and other methods are almost the same, the accuracy of the proposed method is enough. For Case 2, the proposed method can also obtain satisfying results, that is, the accuracy of the proposed method is also enough when non-normally distributed random variables are involved. Compared with the other methods, the total number of LSF evaluations of the proposed method is much less than the ones of other methods. This hence confirms

Table 15 Example 4- Optimization results

	Advanced FORM		Ho-Huu *et al.*(2016)	Proposed method	
	Case 1	Case 2	Case 1	Case 1	Case 2
No. of iterations	31	41	-	27	27
No. of LSF evaluations	95592	121296	170280	10689	10731
d_1^*	0.1000	0.1000	0.100	0.1000	0.1000
d_2^*	0.6821	0.6859	0.682	0.6840	0.6856
d_3^*	0.5353	0.5388	0.533	0.5383	0.5397
d_4^*	0.6642	0.6647	0.661	0.6635	0.6648
d_5^*	0.7371	0.7474	0.727	0.7491	0.7516
d_6^*	0.6692	0.6731	0.670	0.6712	0.6728
d_7^*	0.1000	0.1000	0.100	0.1000	0.1000
d_8^*	0.1000	0.1000	0.100	0.1000	0.1000
d_9^*	1.6683	1.6784	1.665	1.6757	1.6799
d_{10}^*	0.6649	0.6688	0.668	0.6669	0.6685
d_{11}^*	0.1000	0.1000	0.100	0.1000	0.1000
d_{12}^*	0.1000	0.1000	0.100	0.1000	0.1000
d_{13}^*	2.4460	2.4591	2.447	2.4540	2.4600
d_{14}^*	0.6658	0.6697	0.667	0.6678	0.6694
d_{15}^*	0.1000	0.1000	0.100	0.1000	0.1000
d_{16}^*	0.1000	0.1000	0.100	0.1000	0.1000
$\frac{[C_1(\mathbf{d}^*)-\Phi(-3.0)]}{\Phi(-3.0)}$	1.34%	1.73%	1.12%	-1.05%	1.56%
$\frac{[C_2(\mathbf{d}^*)-\Phi(-3.0)]}{\Phi(-3.0)}$	1.56%	1.48%	1.08%	-1.02%	1.41%
$C_0(\mathbf{d}^*)$	479.52	482.16	479.53	481.13	482.25

again the robustness of the proposed method in solving the RBDO problems.

7. Conclusions

An efficient method is presented for solving RBDO problems. It combines the reliability mapping function and an improved surface method. The relationship between a mean value FORM reliability index and an accurate failure probability is called the reliability mapping function. It has been well known that the reliability growth tendency obtained by using different reliability methods should be the same when the design variables are changed. That is, evaluation results obtained by using different reliability methods should be highly correlated. Thus, the reliability mapping function has a clear theoretical basis.

Double-loop involved in the classical RBDO can be converted into single-loop by using reliability mapping functions. Since the computational effort of the mean value FORM is minimal in methods of standard reliability analysis, the efficiency of the proposed method is high. An improved surface method is also proposed to ensure the accuracy of reliability analysis in process of the construction of reliability mapping function. Since the improved response surface method is constructed based on the MPP resulting from the advanced FORM, the accuracy of proposed response surface method should be higher than that of the advanced FORM.

Numerical results reported in this contribution indicated that the proposed method is satisfactory in terms of the total number of LSF evaluations, optimal design, constraints and objective function. Compared with the advanced FORM, the proposed method can obviously reduce the total number of LSF evaluations. In addition, the reliability mapping function does not depend on the selection of sample points, thus the use of reliability mapping function to solve RBDO problems is also feasible.

Numerical results also indicated that the proposed method can obtain the consistent optimization solutions when different LSFs with the same physical meaning are used to construct the reliability mapping function. This illustrates the robustness of the proposed method in solving the RBDO problems. Moreover, the proposed method can also obtain satisfying results when non-normally distributed random variables are involved. This hence confirms again the robustness of the proposed method in solving the RBDO problems.

In this work, since a quadratic polynomial without cross terms is used as a response function, the proposed improved response surface method may be inaccurate for highly non-linear LSFs, the further investigation of the proposed improved response surface method should be required. Although numerical results show that the reliability mapping function is feasible to solve RBDO problems, extensive application of the proposed method to large structural problems with a large number of design variables should be performed in the future.

Acknowledgments

The research described in this paper was financially supported by the Aeronautical Science Foundation of China (Grant No. 2013ZA54004), the General Projects for Liaoning in University of China (Grant No. L2014072), and the Liaoning Provincial Natural Science Foundation of China (Grant No. 201602579).

References

Agarwal, H., Mozumder, C.K., Renaud, J.E. and Watson, L.T. (2007), "An inverse-measure-based unilevel architecture for reliability-based design optimization", *Struct. Multidisc. Optim.*, **33**(3), 217-227.

Chen, Z.Z., Qiu, H.B., Gao, L., Su, L. and Li, P. (2013a), "An adaptive decoupling approach for reliability-based design optimization", *Compu. Struct.*, **117**, 58-66.

Chen, Z.Z., Qiu, H.B., Gao, L., Su, L. and Li, P. (2013b), "An optimal shifting vector approach for efficient probabilistic design", *Struct. Multidisc. Optim.*, **47**(6), 905-920.

Cheng, G., Xu, L. and Jiang, L. (2006), "A sequential approximate programming strategy for reliability-based structural

optimization", *Comput. Struct*., **84**(21), 1353-1367.
Ching, J. and Hsu, W.C. (2008), "Transforming reliability limit-state constraints into deterministic limit- state constraints", *Struct. Saf.*, **30**(1), 11-33.
Cho, T.M. and Lee, B.C. (2011), "Reliability-based design optimization using convex linearization and sequential optimization and reliability assessment method", *Struct. Saf.*, **33**(1), 42-50.
Choi, S.K., Grandhi, R.V. and Canfield, R.A. (2007), *Reliability-based Structural Design*, Springer-Verlag, London, UK.
Ditlevsen, O.D. and Madsen, H.O. (1996), *Structural Reliability Method*, John Wiley & Sons, New York, NY, USA.
Du, X. and Chen, W. (2004), "Sequential optimization and reliability assessment method for efficient probabilistic design", *J. Mech. Des*., **126**(2), 225-233.
Enevoldsen, I. and Sorensen, J.D. (1994), "Reliability-based optimization in structural engineering", *Struct. Saf.*, **15**(3), 169-196.
Fang, J.G., Gao, Y.K., Sun, G.Y. and Li, Q. (2013), "Multiobjective reliability-based optimization for design of a vehicle door", *Finite Elem. Anal. Des.*, **67**, 13-21.
Gasser, M. and Schueller, G.I. (1997), "Reliability-based optimization of structural systems", *Math. Methods Oper. Res.*, **46**(3), 287-307.
Grandhi, R.V. and Wang, L. (1998), "Reliability-based structural optimization using improved two point adaptive nonlinear approximations", *Finite Elem. Anal. Des.*, **29**, 35-48.
Ho-Huu, V., Nguyen-Thoi, T., Le-Anh, L. and Nguyen-Trang, T. (2016), "An effective reliability-based improved constrained differential evolution for reliability-based design optimization of truss structures", *Adv. Eng. Softw.*, **92**, 48-56.
Kharmanda, G, Mohamed, A. and Lemaire, M. (2002), "Efficient reliability-based design optimization using a hybrid space with application to finite element analysis", *Struct. Multidisc. Optim.*, **24**(3), 233-245.
Kirjner-Neto, C., Polak, E. and Kiureghian, A.D. (1998), "An outer approximation approach to reliability-based optimal design of structures", *J. Optim. Theor. Appl.*, **98**(1), 1-16.
Kuschel, N. and Rachwitz, R. (1997), "Two basic problems in reliability-based structural optimization", *Math. Mehods Oper. Res.*, **46**(3), 309-333.
Li, F., Wu, T. and Hu, M. (2010), "An accurate penalty-based approach for reliability-based design optimization", *Res. Eng. Des*., **21**(2), 87-98.
Li, H.S. (2013), "Reliability-based design optimization via high order response surface method", *J. Mech. Sci. Technol*., **27**(4), 1021-1029.
Liang, J., Mourelatos, Z.P. and Tu, J. (2008), "A single-loop method for reliability-based design optimization", *Int. J. Product Develop.*, **5**(1-2), 76-92.
Meng, Z., Li, G., Wang, B.P. and Hao, P. (2015), "A hybrid chaos control approach of the performance measure functions for reliability-based design optimization", *Compu. Struct.*, **146**, 32-43.
Shan, S. and Wang, G.G. (2008), "Reliable design space and complete single loop reliability based design optimization", *Reliab. Eng. Syst. Saf.*, **93**(8), 1218-1230.
Tu, J., Choi, K.K. and Park, Y.H. (1999), "A new study on reliability-based design optimization", *J. Mech. Des.*, **121**(4), 557-564.
Wang, C. and Qiu, Z.P. (2015), "Improved numerical prediction and reliability-based optimization of transient heat conduction problem with interval parameters", *Struct. Multidisc. Optim.*, **51**(1), 113-123.
Wang, C., Qiu, Z.P., Wang, X.J. and Wu, D. (2014), "Interval finite element analysis and reliability-based optimization of coupled structural-acoustic system with uncertain parameters", *Finite Elem. Anal. Des.*, **91**, 108-114.
Yi, P., Cheng, G. and Jiang, L. (2008), "A sequential approximate programming strategy for performance-measure-based probabilistic structural design optimization", *Struct. Saf.*, **30**(2), 91-109.
Youn, B.D., Choi, K.K. and Du, L. (2005), "Adaptive probability analysis using an enhanced hybrid mean value method", *Struct. Multidisc. Optim.*, **29**(2), 134-148.
Yuan, X.K. and Lu, Z.Z. (2014), "Efficient approach for reliability-based optimization based on weighted importance sampling approach", *Reliab. Eng. Syst. Saf.*, **132**, 107-114.
Zhao, W.T. and Qiu, Z.P. (2013), "An efficient response surface method and its application to structural reliability and reliability-based optimization", *Finite Elem. Anal. Des.*, **67**, 34-42.
Zhao, W.T., Shi, X.Y. and Tang, K. (2016), "A response surface method based on sub-region of interest for structural reliability analysis", *Struct. Eng. Mech*., **57**(4), 587-602.
Zou, T. and Mahadevan, S. (2006), "A direct decoupling approach for efficient reliability based design optimization", *Struct. Multidisc. Optim*., **31**(3), 190-200.

CC